The optical exciton-magnon absorption lines in FeF_2 crystals

1993 J. Phys.: Condens. Matter 5 1151

(http://iopscience.iop.org/0953-8984/5/8/017)

J. Phys.: Condens. Matter 5 (1993) 1151–1168. Printed in the UK

The optical exciton–magnon absorption lines in FeF_2 crystals

Taiju Tsuboi† and W Kleemann‡

† Faculty of Engineering, Kyoto Sangyo University, Kamigamo, Kyoto 603, Japan
‡ Angewandte Physik, Universität Duisburg, D-4100 Duisburg 1, Federal Republic of Germany

Received 28 September 1992, in final form 17 November 1992

Abstract. The axial absorption spectra of FeF_2 have been measured at wavelengths between 200 and 3000 nm and temperatures T where $15 < T < 300$ K, to complete previous work, which was restricted to selected wavelength regions. Thirteen absorption bands have been observed at wavelengths longer than 260 nm; these are denoted as A to M in order of increasing energy. Basically they are analysed in terms of excited Fe^{2+} states in a cubic crystal field. Most of these transitions reveal sharp, weak, pure exciton lines at low temperatures. Some of them (E, H1, H2, K) are accompanied by one-magnon cold and hot sidebands. Their moments of order zero and one have the typical temperature dependence predicted by theory. Three-magnon hot sidebands occur within the E and H1 bands. The E_1 line, formerly attributed to a two-magnon transition, *is identified as a pure exciton transition. A double-exciton transition is connected with* the M band at about 300 nm. A weak low-energy satellite of the A band exciton, A′, refers to axial crystal field splitting of the $^5T_{2g}$ ground state.

1. Introduction

Ferrous fluoride FeF_2 has a rutile-type crystal structure and shows three-dimensional Ising-type antiferromagnetism with a Néel temperature T_N of 78.3 K. FeF_2 exhibits several absorption bands in the near-infrared to visible region (McClure *et al* 1967, Tanabe and Gondaira 1967, Chen *et al* 1971, Tylicki and Yen 1968, Kleemann and Uhlig 1989). Most of these bands have a fine structure at low temperatures. The intense lines have been attributed to the exciton–magnon coupled absorption bands (i.e. magnon sidebands), while the very weak lines have been attributed to the zero-magnon, zero-phonon (i.e. pure exciton) lines (Russel *et al* 1966, McClure *et al* 1967, Tanabe and Gondaira 1967, Chen *et al* 1971, Kleemann and Uhlig 1989).

Tylicki and Yen (1968) studied the absorption spectra of the near-infrared bands and found that a hot sideband does not appear. They explained the disappearance of the hot band on the basis of the small thermal population of magnon states because of the large anisotropy gap (about 55 cm^{-1}). If this explanation is true, FeF_2 is expected to have no hot sideband in any absorption band. Recently, Kleemann and Uhlig (1989) studied the temperature dependence of an absorption band located around 465 nm and suggested the presence of a hot band. They, however, have not measured the temperature dependence of the hot-band intensity since it is difficult to estimate the intensity because of overlap with the intense cold band. In this paper we examine the fine structure of the various absorption bands in detail and clarify whether a hot band is present in FeF_2.

0953-8984/93/081151+18$07.50

So far the absorption spectrum due to the electronic transition in Fe^{2+} ions has been reported in limited energy regions (McClure *et al* 1967, Tanabe and Gondaira 1967, Tylicki and Yen 1968, Chen *et al* 1971, Kleemann and Uhlig 1989). An assignment for the observed bands has not been made except for the near-infrared bands. To the best of our knowledge the whole spectrum, which appears below the energy corresponding to the band gap of FeF_2, has not yet been reported. In this paper we present the whole Fe^{2+} absorption spectrum and identify the transitions involved.

2. Experimental procedure and results

A single crystal of FeF_2 cut parallel to the {100} faces (i.e. perpendicular to the c axis) with a thickness of 1.44 mm, which was grown by the Bridgman method, was used for the optical measurement. Unpolarized axial absorption spectra were measured with a Shimadzu UV-3100 spectrophotometer at wavelengths between 200 and 3000 nm in a temperature range of 15–300 K. The spectra were measured at a resolution of 0.1 nm in the 200–850 nm region and of 0.5 nm in the 850–2500 nm region.

Figure 1 shows the absorption spectrum of FeF_2 at 15 K in the 265–2500 nm region. Thirteen intense or weak bands are observed at the low-energy side of an intense absorption edge near 266 nm. They are called A, B, C, D, E, F, G, H, I, J, K, L and M in order of increasing energy. The A band is located in the 1100–1600 nm region at 15 K, and the B band in the 700–1100 nm region. These are much more intense than the other bands. The C band is located at 520–560 nm, the D band at 475–500 nm, the E band at 462–468 nm, the F band at 450–460 nm, the G band at 430–445 nm, the H band at 360–387 nm, the I band at 345–355 nm, the J band at 330–340 nm, the K band at 310–330 nm, the L band at 289–310 nm, and the M band at 270–287 nm.

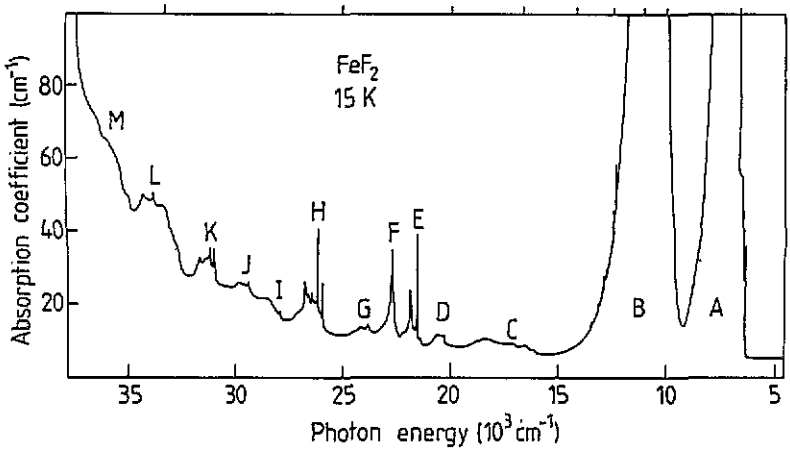

Figure 1. The absorption spectrum of FeF_2 at 15 K.

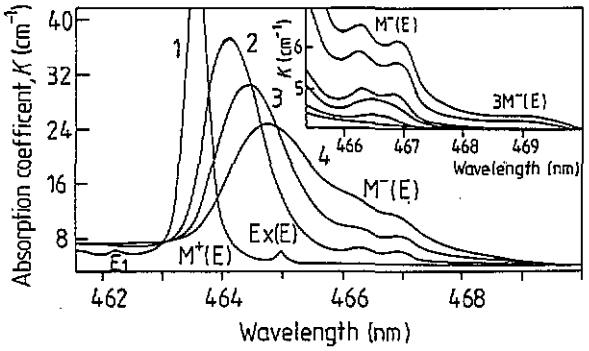

Figure 2. The absorption spectra of the E band in FeF_2 at: 1, 15 K; 2, 62 K; 3, 70 K; and 4, 75 K. The inset shows the enlarged spectra in the 465–470 nm region obtained at (bottom curve upwards) 18, 35, 45, 50, 59 and 62 K.

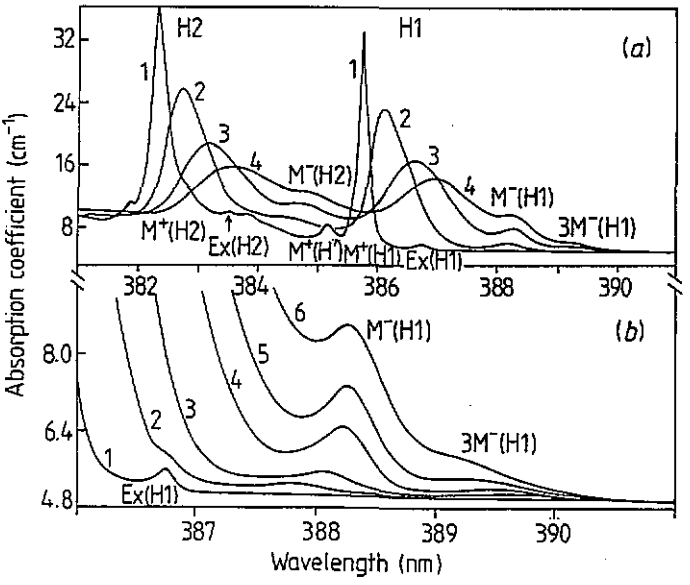

Figure 3. (*a*) The absorption spectra of the H band in FeF_2 at: 1, 15 K; 2, 55 K; 3, 69 K; and 4, 74 K. (*b*) The enlarged spectra of the low-energy tail of the H1 band at: 1, 15 K; 2, 37 K; 3, 48 K; 4, 61 K; 5, 68 K; and 6, 73 K.

Figures 2 and 3 show the temperature dependences of the fine structure of the E and H bands, respectively. At 15 K, an intense and sharp cold band (this band was named M^+ by Kleemann and Uhlig (1989), but we shall call this band $M^+(E)$ hereafter, (see table 1)) is observed at 463.6 nm in the E-band region (figure 2), while a weak exciton band (called Ex(E) hereafter) at 465.0 nm and another weak band (named $2M^+$ by Kleemann and Uhlig (1989), but called $2M^+(E)$ hereafter) at 462.3 nm are observed well separated from the $M^+(E)$ band. As the temperature is increased from 15 K, it is observed that the Ex(E) and $2M^+(E)$ bands vanish, while the $M^+(E)$ band broadens and shifts towards lower energies, in agreement

with the previous measurement (Kleemann and Uhlig 1989). The $M^+(E)$ band is observed to show a large shift at low temperatures below 80 K but a small shift above 80 K, as shown in figure 4. At temperatures above 25 K, a broad hot band is observed to appear in the 466.0–467.5 nm region, which was previously named M^- but is called $M^-(E)$ hereafter. The $M^-(E)$ band has an unstructured lineshape at low temperatures but it begins to develop a doublet structure above about 40 K and has two well resolved peaks above about 52 K (see figures 2 and 4). The $M^-(E)$ band is clearly observed up to 77 K, but it is no longer observed above T_N because of overlap with the intense $M^+(E)$ band. When the temperature is increased up to 55 K, it is observed that another hot band (called $3M^-(E)$) appears at 469.1 nm, as shown in the inset of figure 2.

Table 1. Peak positons of the observed bands in the E-, H- and K-band regions at 15 K and their assignments. Ex, zero-magnon, zero-phonon (i.e. pure exciton) band; M^-, one-magnon hot sideband; $3M^-$, three-magnon hot sideband; M^+, one-magnon cold sideband; MD, magnetic-dipole-allowed transition; ED, electric-dipole-allowed transition.

Band	Peak position (cm^{-1})	Separation (cm^{-1})	Assignment
E band			
$3M^-(E)$	~21 315 (at 58 K)	−186	$3M^-$
$M^-(E)$	~21 431 (at 30 K)	−70	M^-
Ex(E)	21 501 (21 504[a], 21 503(MD)[b])	0	Ex
$M^+(E)$	21 565 (21 568[a] 21 566[b])	+64	M^+
E_1	21 627 (21 631[a])	0	Ex
E_1'	21 674		
E_2'	21 703	+76	M^+
H1 band			
$3M^-(H1)$	~25 660 (at 52 K)	−197	$3M^-$
$M^-(H1)$	~25 789 (at 31 K)	−68	M^-
Ex(H1)	25 857 (25 857[a], 25 857 (MD)[b])	0	Ex
$M^+(H1)$	25 924 (25 927[a], 25 924 (ED)[b])	+69	M^+
Ex(H′)	25 893 (MD)[b]	0	Ex
$M^+(H')$	25 963 (25 964 (ED)[b])	+70	M^+
H2 band			
$M^-(H2)$	~25 994 (at 50 K)	−80	M^-
Ex(H2)	26 074	0	Ex
$M^+(H2)$	26 153 (26 152 (ED)[b])	+79	M^+
K band			
$M^-(K1)$	~30 917	141	M^-
$M^+(K1)$	31 058	141	M^+

[a] Observed by Chen *et al* (1971).
[b] Observed by McClure *et al* (1967).

From the structure of the H band, it seems that the H band is composed of two parts, H1 (the low-energy side, (see figure 3)) and H2 (the high-energy side). Several weak bands are observed at 15 K in addition to the two strong bands at 385.73 and 382.36 nm. Their peak positions are summarized in table 1. As for the case of the $M^+(E)$ band, these strong bands which are called $M^+(H1)$ and $M^+(H2)$,

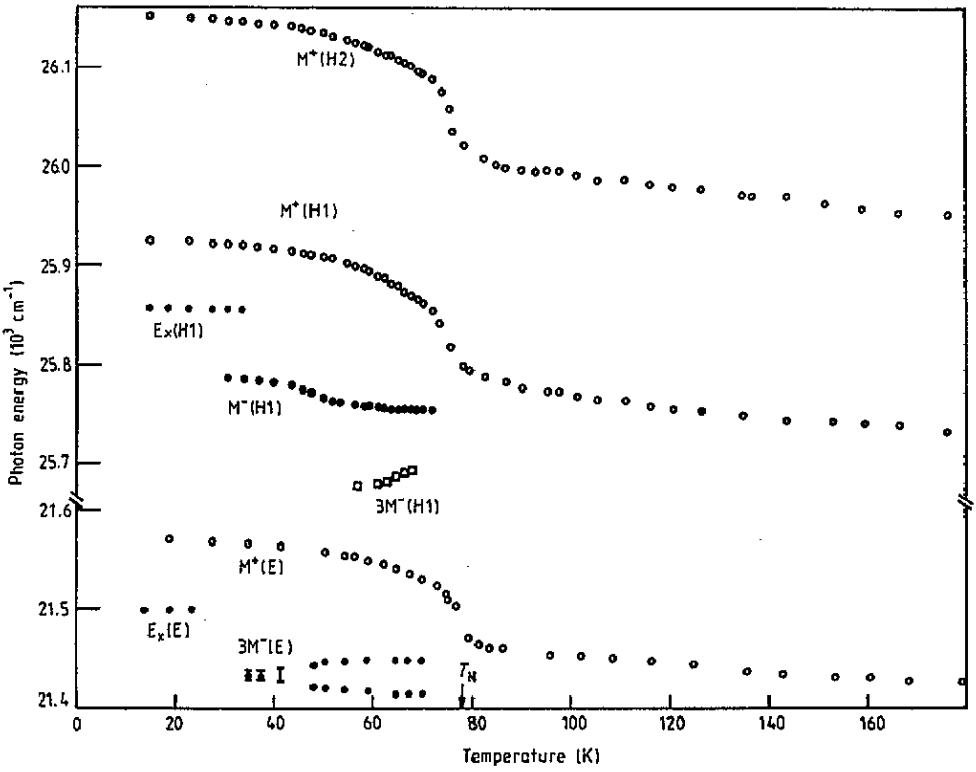

Figure 4. The temperature variation of the peak positions of the cold bands $M^+(E)$, $M^+(H1)$ and $M^+(H2)$ of the exciton band Ex(H1) and of the hot bands $M^-(H1)$, $3M^-(H1)$ and $3M^-(E)$.

respectively, show a red shift with increasing temperature, as shown in figure 3(*a*). The $M^+(H1)$ and $M^+(H2)$ bands are observed to have an asymmetric lineshape, with a steep slope at high energy and a longer tail at low energy at temperatures below about 50 K, as observed for the $M^+(E)$ band. As the temperature is increased from about 30 K, a hot band $M^-(H1)$ begins to grow at the low-energy side of the $M^+(H1)$ band. The $M^-(H1)$ band located at 387.8 nm at 31 K shifts towards low energy with increasing temperature. Similarly, a hot band is observed at the low-energy side of the $M^+(H2)$ band, which is called $M^-(H2)$. Another hot band named $3M^-(H1)$ appears at the low-energy side of the $M^-(H1)$ band above 40 K, as shown in figure 3(*b*), in agreement with the observation by Shapiro and Litvinenko (1975). Unlike the $M^-(H1)$ and $M^-(H2)$ bands, but like the $3M^-(E)$ band, the $3M^-(H1)$ band shows a blue shift (see figures 2 and 4). It is found that the structure, temperature dependence and amount of the peak shift of the H1-region spectrum are quite similar to those of the H2-region spectrum. This is confirmed if we shift the $M^+(H1)$ band to the $M^+(H2)$ band position.

In figure 5 the integrated intensities of the hot bands $M^-(H1)$ and $3M^-(H1)$ are plotted against temperature, together with the integrated intensity of the $M^+(H1)$ band. The temperature dependences of the $M^-(H2)$ and $M^-(E)$ hot bands (not shown) are similar to that of the $M^-(H1)$ band. The same relationship is valid

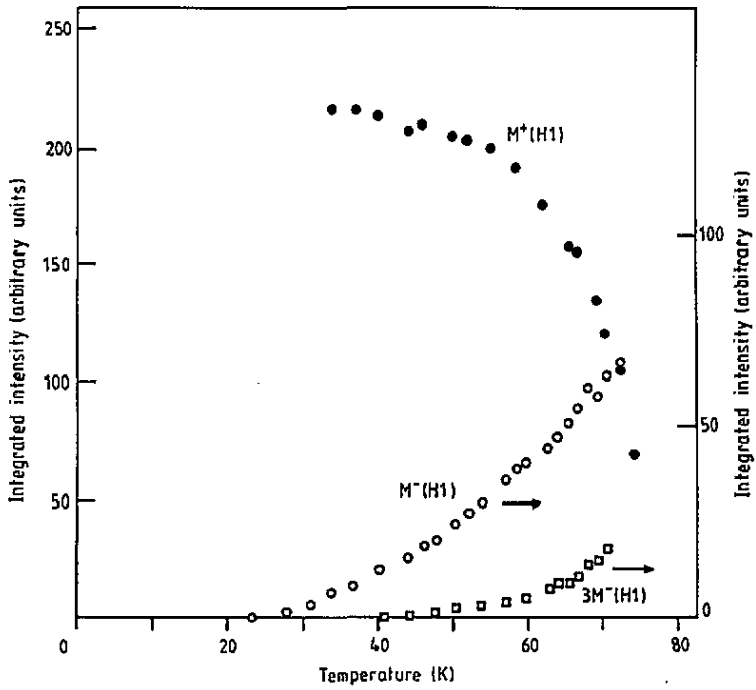

Figure 5. The temperature dependence of the integrated intensities of the hot bands $M^-(H1)$ (open circles, right-hand scale) and $3M^-(H1)$ (open squares, right-hand scale) and of the cold band $M^+(H1)$ (full circles, left-hand scale).

between $M^+(H1)$ and $M^+(H2)$.

An intense, sharp line with associated fine structure is observed at the low-energy side of the A band, as observed by Tylicki and Yen (1968). The sharp line is located at 1566 nm at 14 K, and is called Ex(A). As the temperature is increased from 14 K, the peak height of the Ex(A) band increases with increasing temperature, but it decreases above about 40 K, as shown in figure 6. Above 100 K the Ex(A) band is too weak to be accurately identified. As shown in figure 7, its intensity (i.e. integrated intensity) increases in the temperature region 14–40 K, while it decreases above 40 K. It is observed for the first time that a weak band appears at around 1573 nm above 19 K. The new band is called the A′ band (see figure 6). Although the A′ band is not well resolved from the Ex(A) band, it is observed growing with increasing temperature (figure 7). The Ex(A) band shows a broadening and a peak shift to low energy with increasing temperature. The temperature dependence of the peak shift is shown in figure 7.

The D band has a fine structure with two relatively sharp peaks (at 492.1 and 490.8 nm) at the low-energy side, accompanied by several small and unresolved peaks at the high-energy side. When the temperature is increased, the 492.1 and 490.8 nm bands decrease their peak height and become broad quickly, and the fine structure is smeared out at temperatures above 50 K, as shown in figure 8. No absorption band is observed at the low-energy side of the 492.1 nm band with increasing temperature.

A sharp line (called the α band) is observed at 809.5 nm in the high-energy tail

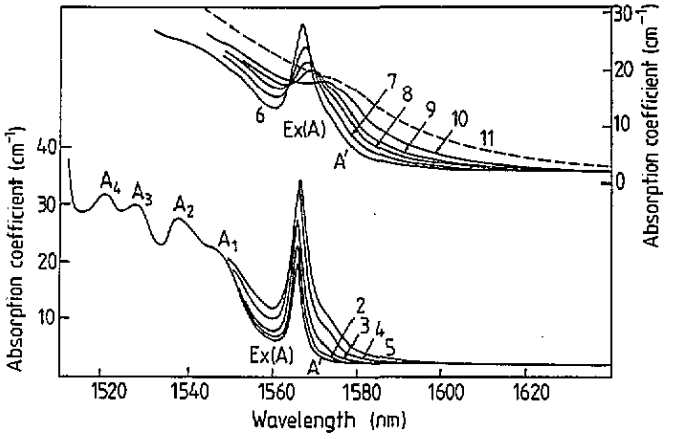

Figure 6. The absorption spectra of the low-energy side of the spin-allowed A band at: 1, 14 K; 2, 19 K; 3, 25 K; 4, 33 K; 5, 39 K; 6, 45 K; 7, 53 K; 8, 59 K; 9, 63 K; 10, 74 K; and 11, 95 K.

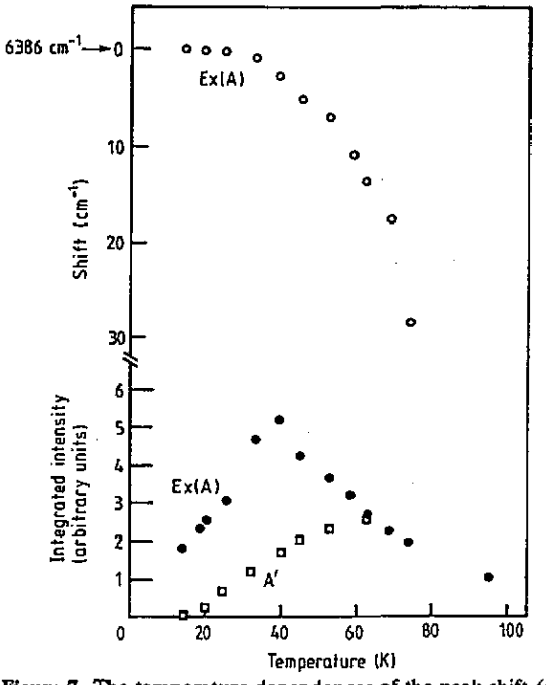

Figure 7. The temperature dependences of the peak shift (open circles) and the integrated intensity (full circles) of the Ex(A) band, together with the integrated intensity (open squares) of the A′ band. The latter intensity is magnified by a factor of ten.

of the intense B band. The a band has an asymmetric lineshape whose high-energy part is broader than the low-energy part. At the high-energy side of the a band, a fine structure with a very weak intensity is observed, as shown in figure 9: its components are called b, c, d, e, f, g, h and i bands. These a–i bands exhibit the same temperature dependence as each other. A typical temperature dependence is

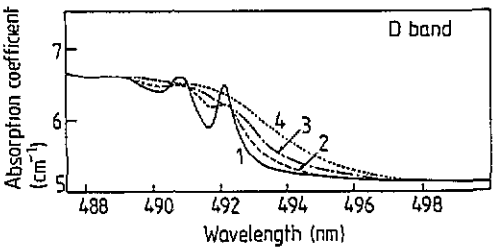

Figure 8. The absorption spectra at the low-energy side of the D band measured at: 1, 15 K; 2, 41 K; 3, 51 K; and 4, 65 K.

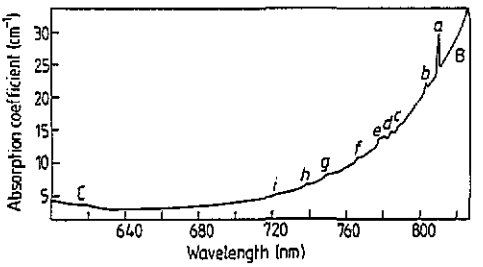

Figure 9. The absorption spectrum at the high-energy tail of the B band at 15 K.

shown for the *a*, *d* and doublet-structured e bands in figure 10. The intensity of each band decreases monotonically with increasing temperature (figure 11). All the bands disappear above 70 K. Such a temperature dependence is different from that of a magnon cold sideband like the $M^+(E)$ band, but it is similar to an exciton band like the Ex(E) band.

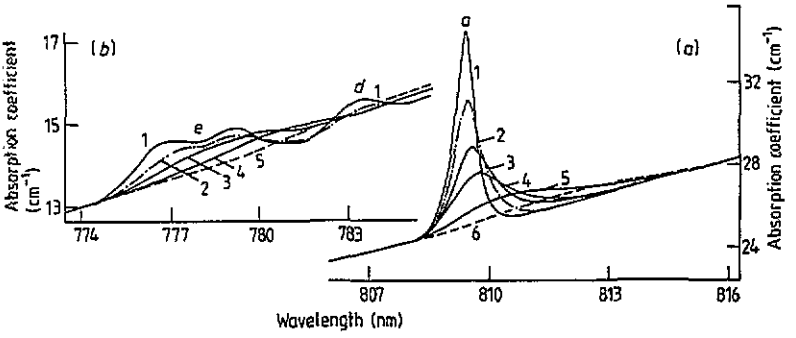

Figure 10. The absorption spectra of (*a*) the *a* band measured at: 1, 15 K; 2, 26 K; 3, 33 K; 4, 42 K; 5, 54 K; and 6, 67 K; and (*b*) the *d* and *e* bands measured at: 1, 15 K; 2, 36 K; 3, 50 K; 4, 64 K; and 5, 100 K.

3. Energy level assignment

The energy diagram of the Fe^{2+} ion in a cubic crystal field has been calculated by Kambara (1968). In 1968 only the absorption spectra in the A-, B- and H-band regions were available in FeF_2. Kambara estimated values of 825 and 660 cm^{-1} for the Racah parameter B and the cubic field parameter Dq, respectively, to fit the zero-magnon lines of the A and H bands. We have obtained a nearly complete absorption spectrum associated with the crystal field splitting of Fe^{2+} (figure 1), therefore we can check whether the estimate of $Dq/B = 0.80$ is correct. In figure 12 we show the calculated energy diagram and compare the absorption spectrum at 15 K. Kambara (1968) obtained the diagram in a Dq/B region of 0 to 2.0, but we have shown a limited region of 0 to 0.80 in figure 12. A quite good agreement between the

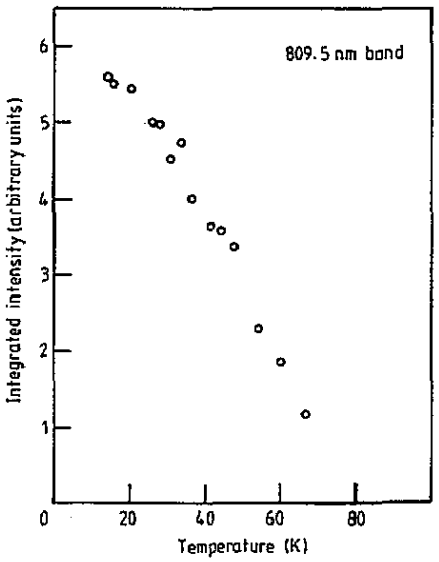

Figure 11. The temperature dependence of the integrated intensity of the α band.

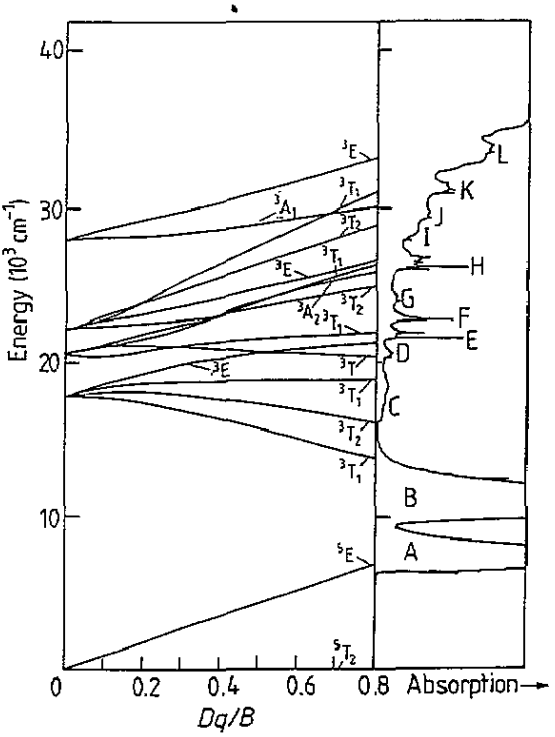

Figure 12. The energy diagram for Fe^{2+} in a cubic crystal field, calculated by Kambara (1968), compared with the electronic absorption spectrum of FeF_2 at 15 K.

absorption bands and the energy levels at $Dq/B = 0.80$ is found for almost all the absorption bands. Although a detailed level assignment using the energy diagram of figure 12 is not possible, because the symmetry of the Fe^{2+} ion is not cubic in FeF_2

but D_{2h} in the paramagnetic phase and C_{2h} in the antiferromagnetic phase, we can identify the observed near-infrared to ultraviolet absorption bands using the energy diagram to a first-order approximation.

The A and B bands have been assigned to the spin-allowed $^5T_{2g} \rightarrow {}^5E_g$ transition (Tylicki and Yen 1968). They are widely separated from each other (the separation is about 3500 cm^{-1}) by a strong Jahn–Teller interaction of the ^5E_g state with lattice vibrations (Jones 1967, Tylicki and Yen 1968). The two bands are considerably stronger than the other bands which are due to the spin-forbidden transitions (figure 1). Therefore the previous assignments for the A and B bands are confirmed to be correct.

Absorption bands associated with the transition from the ground $^5T_{2g}$ state to the lowest triplet state $^3T_{1g}(1)$ are expected to be weak, as for the cases of the other spin-forbidden C to L bands. In the high-energy tail of the B band, we observed a weak but sharp line at 809.5 nm accompanied by a fine structure at its high-energy side (figure 9). Unlike the A and B bands, the a–i bands become small with increasing temperature. This indicates that these bands do not originate from the same transition as the spin-allowed B band, although they are superposed on the B band. The energies of the 809.5 nm line and the accompanying weak bands are not far from the energy of the $^3T_{1g}(1)$ level (13 700 cm^{-1}), which was estimated at $Dq/B = 0.80$. Therefore a group of the a–i bands is attributable to the spin-forbidden transition to the $^3T_{1g}(1)$ state.

We have observed a broad band as the C band. Taking into account that the C band has a fine structure, the C band is suggested to be composed of two bands: a low-energy band due to the transitions to the $^3T_{2g}(1)$ state; and a high-energy band corresponding to the $^3T_{2g}(2)$ state. The observed H band consists of many sharp lines. The energy diagram suggests that three energy levels, $^3A_{2g}(1)$, $^3T_{1g}(4)$ and $^3E_g(2)$, in order of increasing energy, are responsible for the composite H band. Thus we suggest that the H1 and H2 bands are attributable to the transition to the $^3A_{2g}(1)$ and $^3T_{1g}(4)$ states, respectively, while the high-energy component is due to the $^3E_g(2)$ state.

Similarly, we can assign the other absorption bands: the D, E, F, G, I, J, K and L bands to the spin-forbidden transition from the $^5T_{2g}$ state into the $^3T_{2g}(2)$, $^3E_g(1)$, $^3T_{1g}(3)$, $^3T_{2g}(3)$, $^3T_{2g}(4)$, $^3A_{1g}$, $^3T_{1g}(5)$ and $^3E_g(3)$ states, respectively. According to the calculated energy diagram, it is expected that no Fe^{2+} absorption appears in the 33 000–46 000 cm^{-1} region, but several spin-forbidden Fe^{2+} absorption bands appear in the 46 000–51 000 cm^{-1} region. We cannot confirm this prediction since a much more intense absorption, which appears to be caused by charge transfer from the F^- to Fe^{2+} ions, appears in the high-energy region, above about 36 000 cm^{-1}.

There is no Fe^{2+} energy level which corresponds to the M band. The M band is believed to be caused by a double-exciton transition, which has been observed in, for example, $BaMnF_4$ (Tsuboi and Kleemann 1983). The M band is suggested, for example, from the point of view of the photon-energy value, to be the $^3T_{1g}(2) + {}^3T_{1g}(2)$ band, where the $^3T_{1g}(2)$ level corresponds to the high-energy component of the C band. We have not confirmed this conjecture from the temperature dependence because it is difficult to estimate precisely the intensity, because of the overlap with the intense charge-transfer absorption located at the high-energy side.

4. Discussion

4.1. One-magnon and three-magnon hot sidebands

As was achieved by Kleemann and Uhlig (1989), the temperature-(T-) dependent $M^-(E)$ band is attributable to the one-magnon hot band associated with the exciton line Ex(E) from the $M^-(E)$–Ex(E) separation. A three-magnon hot band has been predicted theoretically (Fujiwara and Tanabe 1972). We have confirmed its existence experimentally in $BaMnF_4$ (Tsuboi and Kleemann 1983). The observed T-dependent band $3M^-(E)$ is assigned to the three-magnon hot band since the separation from the Ex(E) band is about three times that of the Ex(E)–$M^-(E)$ separation. The relative T-dependence of the band intensities (figure 5) is quite similar to the theoretically calculated T-dependence of three-magnon and one-magnon hot bands which was made for $RbMnF_3$ by Fujiwara and Tanabe (1972). Therefore, taking into account the fact that the lower-energy band $3M^-(E)$ begins to appear at higher temperatures than the higher-energy band $M^-(E)$, we can assign the $M^-(E)$ and $3M^-(E)$ bands to the one- and three-magnon hot bands associated with the exciton band Ex(E) (see table 1). Similarly, by comparing the theoretically expected properties of the one- and three-magnon hot bands, the $M^-(H1)$ and $3M^-(H1)$ bands are assigned to the one- and three-magnon hot bands associated with the Ex(H1) exciton line, respectively, and the $M^-(H2)$ band to the one-magnon hot band associated with the Ex(H2) exciton line (see figure 4). The three-magnon hot band associated with the Ex(H2) exciton was not found, presumably because of the superposition with the intense cold band $M^+(H1)$.

When the hot-band intensity is plotted against temperature in a log–log scale, it is found that it obeys approximately the following relation:

$$I(T) = aT^d \tag{1}$$

with $d = 3.0$ for the one-magnon hot band $M^-(H1)$ and $d = 7.1$ for the three-magnon hot band $3M^-(H1)$, where a is a constant. The T-dependence of the one-magnon hot band intensity has been known to depend on the magnetic dimensionality: the d-value of relation (1) is approximately $d = 1$, 2 and 3 for the one-, two- and three-dimensional magnets (Tsuboi 1984, Day 1985, Eremenko *et al* 1988, Tsuboi and Ahmet 1992). Thus our present case unequivocally confirms that FeF_2 is classified as a three-dimensional antiferromagnet. Regarding the three-magnon hot band, a theoretical T-dependence has been calculated for the case of the three-dimensional antiferromagnet $RbMnF_3$ by Fujiwara and Tanabe (1972). From a log–log plot of the theoretical T-dependence of the hot-band intensity, we estimate that $d = 7.3$ for $RbMnF_3$. This value is close to our value, $d = 7.1$. Therefore, the assignment of the $3M^-(H1)$ band to the three-magnon hot band is confirmed to be reasonable.

Among the three electric-dipole-allowed magnon sidebands, including two hot bands (one-magnon and three-magnon hot bands) and a cold band (one-magnon band), which are allowed in antiferromagnets (Shinagawa and Tanabe 1971, Fujiwara and Tanabe 1972), the cold band is considerably stronger than the other ones and is located by the zone-edge magnon energy (77 cm^{-1} (Fleury *et al* 1966, Hutchings *et al* 1970)) above the magnetic-dipole-allowed exciton band. According to their separation from the exciton band, the intense $M^+(E)$ and $M^+(H1)$ bands are assigned to the one-magnon cold band, in agreement with previous assignments (Chen *et al* 1971, Kleemann and Uhlig 1989). Another intense band $M^+(H2)$ is also assigned to the

cold band. These cold bands decrease with increasing temperature and the rate of decrease becomes large as the temperature approaches T_N. The behaviour is quite similar to the case of MnF_2 (Tsuboi and Ahmet 1992), which is consistent with the theoretical result calculated for the cold band in MnF_2 and $RbMnF_3$ (Shinagawa and Tanabe 1971, Fujiwara and Tanabe 1972). Thus the assignment for the $M^+(E)$, $M^+(H1)$ and $M^+(H2)$ bands is confirmed to be reasonable. In table 1 the assignments for the observed bands in the E- and H-band regions are summarized.

In figure 13 we show the temperature dependence of the peak shift of the one-magnon cold sidebands $M^+(E)$ and $M^+(H1)$ with respect to their positions at 15 K, comparing these with the shift of the two-magnon Raman line obtained by Fleury (1970). It is noted that the shift of the $M^+(H1)$ sideband is the same as the other one-magnon sideband $M^+(H2)$ (not shown in figure 13) but not the same as the $M^+(E)$ sideband. This indicates that the amount of shift of the sideband depends on the exciton state concerned. Additionally, the shift of these sidebands is similar to the Raman shift, but the amount of shift of the $M^+(H1)$ and $M^+(H2)$ sidebands is not in agreement with the Raman shift at temperatures above about 75 K.

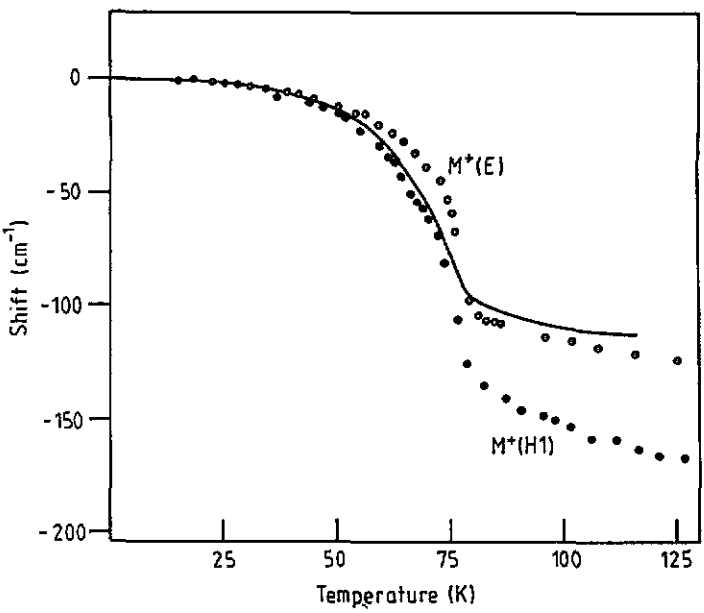

Figure 13. The temperature dependence of the peak shifts of the cold bands $M^+(H1)$ (full circles) and $M^+(E)$ (open circles), compared with the peak shift of the two-magnon Raman band (full curve) obtained by Fleury (1970).

4.2. Two-magnon cold sideband?

The E_1 band observed at 462.25 nm (figure 2) has been suggested to be assigned to the two-magnon sideband by Chen *et al* (1971). Two reasons have been given

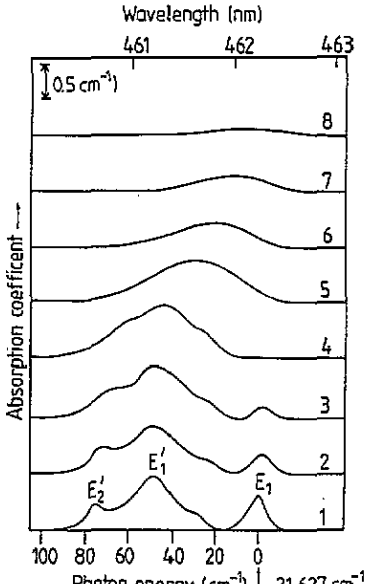

Figure 14. The absorption spectra of the E_1 and E′ bands observed at the high-energy side of the E band, measured at: 1, 15 K; 2, 27 K; 3, 35 K; 4, 41 K; 5, 59 K; 6, 65 K; 7, 70 K; and 8, 73 K.

for this assignment: (i) it is located at 127 cm^{-1} above the exciton line Ex(E) at 21 504 cm^{-1} (corresponding to our 21 501 cm^{-1} line), the energy separation from the exciton line being near to the energy of the two-zone-edge magnons at 154 cm^{-1}; and (ii) the thermal shift is in good agreement with the thermal shift of the two-magnon Raman band. However, the two-magnon cold sideband in antiferromagnets is not allowed for the electric dipole transition in the two-sublattice antiparallel Fe^{2+} spin system. Therefore Chen *et al* (1971) have indicated that the E_1 band is allowed by the electric dipole transition in a three-centre model where two magnons are created on one sublattice and a zone-centre exciton is created on the other. The E_1 band has a half-width of 8 cm^{-1} at 15 K, which is considerably smaller than that of the one-magnon cold band $M^+(E)$, but close to the half-width of 7 cm^{-1} for the Ex(E) band. However, a broad band is expected for the multi-magnon sideband, as in the case of $RbMnF_3$ where the three-magnon sideband is expected to be a single band with a width of 20–30 cm^{-1} (Fujiwara and Tanabe 1972). Additionally, the peak height of the E_1 band decreases with increasing temperature, just as for the exciton band. The peak height disappears above about 40 K, but the two-magnon Raman band never disappears, even at high temperatures above 40 K (Cottam *et al* 1983). A two-magnon cold sideband has been observed in $RbMnF_3$, in addition to two three-magnon sidebands (Eremenko and Petrov 1977). However, unlike the three-magnon bands, the two-magnon band appears only under an external magnetic field. The E_1 band of FeF_2 is observed at zero field. Therefore, we do not believe that the above-mentioned reasons never give any other choice than Chen *et al*'s assignment of the E_1 band.

We examined the absorption spectra in the vicinity of the E_1 band, to support an alternative interpretation of the E_1 band. A broad band is located in a region of 20–85 cm^{-1} energy above the E_1 band at 15 K, as shown in figure 14. The band (called the E′ band) is larger than the E_1 band. The E′ band has a fine structure at low temperatures, with two peaks named E'_1 and E'_2 at 461.25 and

460.64 nm, respectively, but the doublet-like structure becomes smeared out with increasing temperature, showing a shift towards lower energy. The thermal shift is almost the same as for the one-magnon cold band $M^+(E)$ (figure 15). Additionally, the temperature dependence of the E′-band intensity is similar to that of the M^+ band (figure 15). This behaviour indicates that the E′ band is attributable to a cold-magnon sideband. The high-energy edge E_2' in the E′ band is located at 76 cm^{-1} *from the* E_1*-band position, whose separation is close to the magnon energy. This* suggests that the E′ band is a one-magnon cold sideband associated with an exciton line, i.e. the E_1 band. Therefore it is natural to attribute the E_1 band to the exciton rather than to the two-magnon transition. The E′ band has a large peak (named E_1') at 29 cm^{-1} below the high-energy edge E_2'. Such a fine structure for the E′ band may be explained by the magnon dispersion.

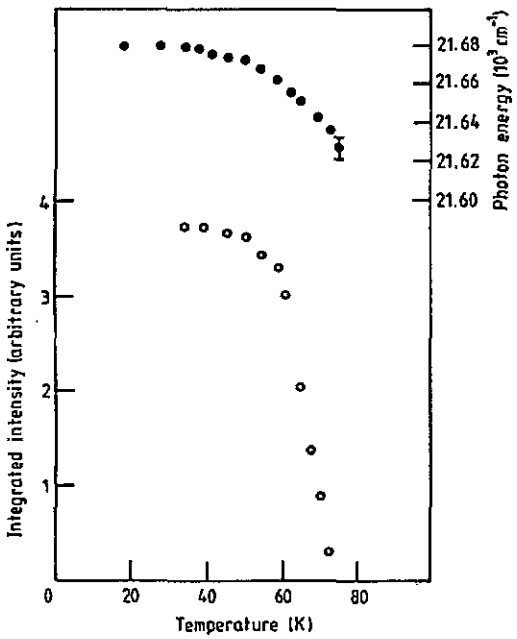

Figure 15. The temperature variation of the peak positions and integrated intensity of the E′ band.

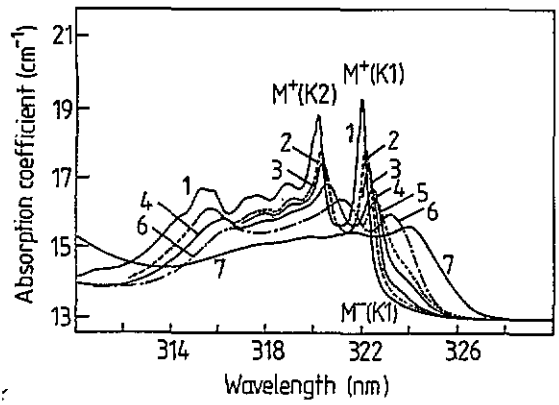

Figure 16. The absorption spectra of the K band measured at: 1, 15 K; 2, 48 K; 3, 55 K; 4, 66 K; 5, 70 K; 6, 76 K; and 7, 205 K.

The hot $M^-(E)$ sideband has a doublet structure. The separation of the two components is about 30 cm^{-1}, which is close to the separation of the E_1' and E_2' peaks. Therefore, taking into account the similarity of the structure between the $M^-(E)$ and E′ bands, our assignment of the E_1 band to the exciton line is reasonable.

A doublet-structured cold-magnon sideband has been observed in the quasi-two-dimensional antiferromagnet $(C_2H_5NH_3)_2MnCl_4$ (Kojima *et al* 1976, 1978). The separation between the two components is 46.4 cm^{-1}, which is bigger than the E_1'–E_2' separation. As for the case of our E′ band, the doublet structure becomes smeared out with increasing temperature. The lineshape has been explained by taking into account the magnon dispersion and the exciton dispersion due to inter- and intra-sublattice exciton transfers (Kojima *et al* 1978). According to the calculation for the absorption band using various values for the inter- and intra-sublattice transfer constants, a lineshape with a higher peak at low energy is obtained by increasing the value of the intra-sublattice transfer constant. We have not calculated the lineshape of the magnon sideband of FeF_2 because the detailed exciton dispersion is unknown, but it is believed to be possible to derive the theoretical lineshape in agreement with the experimental one of figure 14. The presence of an exciton transfer has been suggested in MnF_2 (see, for example, Fujiwara and Tanabe 1972, Wilson *et al* 1979). The crystal structure and magnetic properties of MnF_2 resemble those of FeF_2. Therefore, it is conceivable that the exciton transfer is also present in FeF_2, and it has an essential effect on the lineshape of the magnon sideband.

4.3. The fine structure of the K band

The K band has two sharp lines on the low-energy side at 321.97 and 320.06 nm at 15 K; these are named $M^+(K1)$ and $M^+(K2)$ bands, respectively. These two lines shift towards low energy with increasing temperature, as shown in figure 16. Figure 17 shows the T-dependence of the peak position and half-width of the $M^+(K1)$ band. The T-dependence of the shift (including the amount of the shift) is the same in the $M^+(K1)$ and $M^+(K2)$ bands in the temperature range measured (15–250 K) and it is also the same as that of the $M^+(H1)$ band. A cusp-like sharp peak appears at about T_N in the half-width, just as observed for the $M^+(E)$ band (Kleemann and Uhlig 1989). This behaviour is similar to that predicted theoretically for the one-magnon cold band in $RbMnF_3$ by Shinagawa and Tanabe (1971). Not only the T-dependence of the peak shift and half-width but also the T-dependence of the intensity are similar to the $M^+(H1)$ band, indicating that the $M^+(K1)$ and $M^+(K2)$ bands are attributable to the cold sideband. We tried to find an exciton line associated with the cold band, which is expected to be located around 75 cm^{-1} below the $M^+(K1)$ band. No sharp line was revealed, presumably since it would be immersed under the tail of the $M^+(K1)$ band because of its weak intensity, but an unresolved weak band (named $M^-(K1)$) was observed to appear at about 323.4 nm, and to grow with increasing temperature, as shown in figure 13. The separation of the $M^+(K1)$ band and the $M^-(K1)$ band is about 141 cm^{-1}, which is close to the distance between the one-magnon cold band and the one-magnon hot band. Therefore the T-sensitive $M^-(K1)$ band is attributable to the one-magnon hot band.

At the high-energy tail of the intense $M^+(H1)$ band, a weak band is observed at 385.16 nm at 15 K which is named $M^+(H')$ (figure 3). The $M^+(H')$ band shifts towards low energy and decreases with increasing temperature. The T-dependence of the peak shift and intensity is similar to that of the $M^+(H1)$ band. Taking into account that it is due to an electric-dipole-allowed transition (McClure *et al* 1967), the

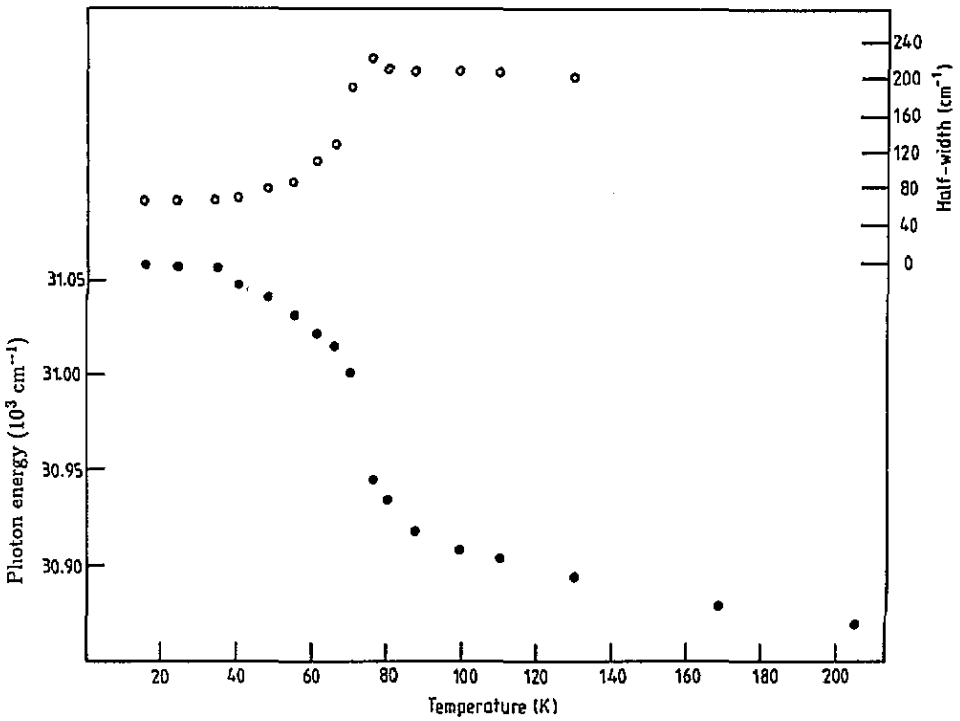

Figure 17. The temperature dependence of the peak position (full circles, left-hand scale) and half-width (open circles, right-hand scale) of the 321.97 nm $M^+(K1)$ band.

$M^+(H')$ band is attributable to the cold sideband. A very weak, sharp and magnetic-dipole-allowed line has been observed at 386.09 nm in the σ-polarization (McClure *et al* 1967, Tanabe and Gondaira 1967). The separation between the exciton-like 386.09 nm line (named Ex(H')) and the $M^+(H')$ band is 70 cm^{-1}, which is close to the magnon energy. Thus the $M^+(H')$ band is concluded to be the one-magnon cold sideband associated with the Ex(H') exciton band, in agreement with the assignment by Tanabe and Gondaira (1967).

4.4. Spin-allowed transitions

The Ex(A) band at 6382 cm^{-1} has been assigned to the zero-phonon, zero-magnon line, i.e. to the pure exciton band (Tylicki and Yen 1968, Moriya and Inoue 1968). The peak of the Ex(A) band has an absorption coefficient of 15.10 cm^{-1} at 15 K. However, the exciton band Ex(E) has a peak height of absorption coefficient 1.60 cm^{-1}, and another exciton band, Ex(H1), has one of 0.40 cm^{-1}. The reason why the Ex(A) band is considerably stronger than the other exciton bands is that the former is due to the spin-allowed $^5T_{2g} \rightarrow {}^5E_g$ transition, while the latter transitions are spin forbidden.

The Ex(A) band is similar to the exciton bands Ex(E) and Ex(H1) with respect to the sharp lineshape. The Ex(A) band, however, is different from the latter bands in the following way. As the temperature is increased from 15 K, the peak heights of the Ex(E), Ex(H1) and Ex(H2) exciton bands decrease and their half-widths increase, resulting in invariance of their integrated intensities versus temperature. Contrastingly, the Ex(A) band shows a broadening and an increase of the peak

height already in the temperature region limited to 14–40 K, resulting in an increase of the integrated intensity. In addition, as remarked above, the Ex(A) band is much more intense than the Ex(E) and Ex(H1) bands: it is approximately 10 and 35 times more intense than the Ex(E) and Ex(H1) bands, respectively.

In parity-forbidden but spin-allowed transitions, like the $^5T_{2g} \rightarrow {}^5E_g$ transition, phonon effects are usually important. In fact, it has been observed in many magnetic insulators that the intensity f of the absorption bands due to such a transition is described by $f(T) = f(0)\coth(h\nu/2kT)$, where h is Planck's constant and ν is the effective frequency of the vibration (see, for example, Ballhausen 1962, Tsuboi *et al* 1985, Tsuboi and Iio 1985). The increase in intensity of the Ex(A) band observed in the temperature region 14–40 K is, hence, understood to be caused by phonon effects.

A weak band A′ is hardly observed at temperatures below 15 K but it grows above 19 K with increasing temperature. Such a hot-band-like band probably does not correspond to the one-magnon hot sideband although it appears at the low-energy side near the exciton band Ex(A), because the separation of the A′ and Ex(A) bands is only 29 cm^{-1}. This is considerably smaller than the magnon energy of 77 cm^{-1}. We believe that the origin of the A′ band is understood within a single-ion model. The ground state $^5T_{2g}$ of Fe^{2+} is split into several levels by the spin–orbit interaction and by the crystal field. The first excited level in the $^5T_{2g}$ state is populated with increasing temperature. If the lowest excited level lies 29 cm^{-1} above the ground level, the transition from the first excited level to the upper ^5E_g state of the Fe^{2+} is expected to become enhanced with increasing temperature, giving rise to the A′ band.

The $^5T_{2g}$ state is split into three levels ($^5T_{21}$, $^5T_{22}$ and $^5T_{23}$ in order of increasing energy, as named by Prinz (1980)) by the spin–orbit interaction in a cubic crystal field. The lowest excited level $^5T_{22}$ is at 2λ above the ground level $^5T_{21}$, where λ is the free-ion spin–orbit coupling constant. Since the coupling constant is about 100 cm^{-1} (Prinz 1980), the A′ band is not attributable to the transition from the $^5T_{22}$ state to the upper ^5E_g state. The ground state $^5T_{21}$ is further split by the C_{2h} crystal field distortion which exists in FeF_2 below T_N. For the case of $RbFeCl_3$, the $^5T_{21}$ state is split into two levels by a trigonal field distortion, with a separation of 12 cm^{-1} (Prinz 1980). This separation is much closer to the A′–Ex(A) separation than the spin–orbit separation of the $^5T_{21}$ and $^5T_{22}$ levels. Therefore, it is suggested that the A′ band is attributable to the transition from the first excited level which originates from the low-symmetry crystal field splitting of the $^5T_{21}$ state.

5. Conclusion

From the experimental results for the absorption bands due to the electronic transitions of the Fe^{2+} ions we have obtained new information on the exciton and magnon sideband in FeF_2, extending previous work of Kleemann and Uhlig (1989). The presence of hot-magnon sidebands in FeF_2 has been confirmed by the observation of the one-magnon and three-magnon hot bands in the E and H bands. Additionally, from a comparison with previous ligand field calculation, it is confirmed that the observed A-L bands are attributable to the excited Fe^{2+} states in a cubic crystal field.

Acknowledgments

The present work is partially supported by the Grants-in-Aid from the Japanese Ministry of Education and Science. This work is also partially supported by the Deutsche Forschungsgemeinschaft through 'Sonderforschungsbereich 166'.

References

Ballhausen C J 1962 *Introduction to Ligand Field Theory* (New York: McGraw-Hill)
Chen M Y, Scarpace F L, Passow M W and Yen W M 1971 *Phys. Rev.* B **4** 132–5
Cottam M G, So V, Lockwood D J, Katiyar R S and Guggenheim H J 1983 *J. Phys. C: Solid State Phys.* **18** 6059–62
Day P 1985 *Phil. Trans. R. Soc.* A **314** 145–58
Eremenko V V, Litvinenko Yu G and Matyushkin E V 1988 *Spin Waves and Magnetic Excitations* vol 1, ed A S Borovik-Romanov and S K Sinha (New York: Elsevier) ch 3
Eremenko V V and Petrov E G 1977 *Adv. Phys.* **26** 31–78
Fleury P A 1970 *J. Appl. Phys.* **41** 886–8
Fleury P A, Porto S P S, Cheesman L E and Guggenheim H J 1966 *Phys. Rev. Lett.* **17** 84–7
Fujiwara T and Tanabe Y 1972 *J. Phys. Soc. Japan* **32** 912–26
Hutchings M T, Rainford B D and Guggenheim H J 1970 *J. Phys. C: Solid State Phys.* **3** 307–22
Jones G D 1967 *Phys. Rev.* **155** 259–61
Kambara T 1968 *J. Phys. Soc. Japan* **24** 1242–50
Kleemann W and Uhlig R 1989 *J. Phys.: Condens. Matter* **1** 1653–61
Kojima N, Ban T and Tsujikawa I 1976 *J. Phys. Soc. Japan* **41** 1809–10
—— 1978 *J. Phys. Soc. Japan* **44** 923–9
McClure D S, Meltzer R, Reed S A, Russel P and Stout J W 1967 *Optical Properties of Ions in Crystals* ed H M Crosswhite and H W Moos (New York: Interscience) pp 257–77
Moriya T and Inoue M 1968 *J. Phys. Soc. Japan* **24** 1251–64
Prinz G A 1980 *J. Magn. Magn. Mater.* **15–18** 839–40
Russel P G, McClure D S and Stout J W 1966 *Phys. Rev. Lett.* **16** 176–8
Shapiro V V and Litvinenko Yu G 1975 *Sov. J. Low Temp. Phys.* **1** 621–2
Shinagawa K and Tanabe Y 1971 *J. Phys. Soc. Japan* **30** 1280–91
Tanabe Y and Gondaira K 1967 *J. Phys. Soc. Japan* **22** 573–81
Tsuboi T 1984 *Phys. Lett.* A **102** 138–40
Tsuboi T and Ahmet P 1992 *Phys. Rev.* B **45** 468–70
Tsuboi T, Chiba M and Ajiro Y 1985 *Phys. Rev.* **32** 354–9
Tsuboi T and Iio K 1985 *J. Phys. C: Solid State Phys.* **18** 6059–62
Tsuboi T and Kleemann W 1983 *Phys. Rev.* B **27** 3762–79
Tylicki J and Yen W M 1968 *Phys. Rev.* **166** 488–94
Wilson B A, Yen W M, Hegarty J and Imbusch G F 1979 *Phys. Rev.* **19** 4238–50